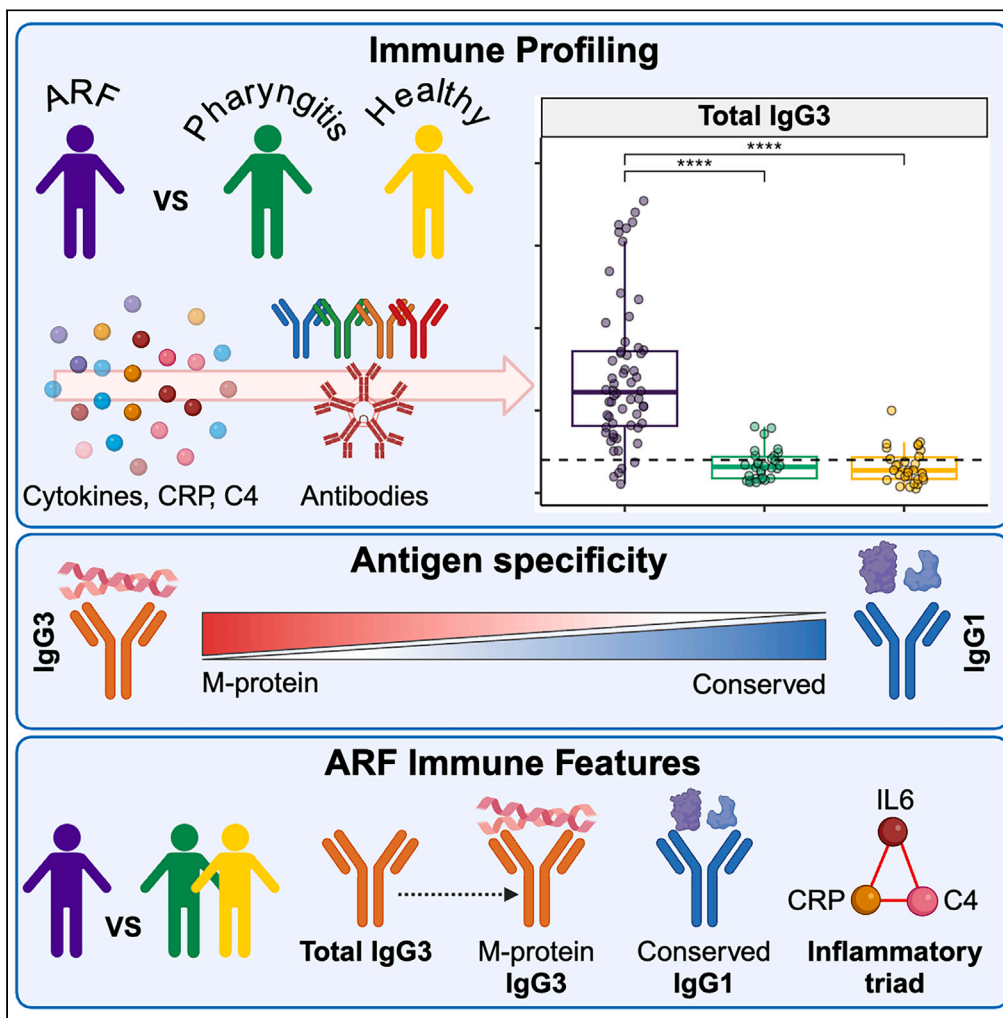**CellPress**

Article

An acute rheumatic fever immune signature comprising inflammatory markers, IgG3, and *Streptococcus pyogenes*-specific antibodies

Natalie Lorenz, Reuben McGregor, Alana L. Whitcombe, ..., Nigel J. Wilson, Amy W. Chung, Nicole J. Moreland

n.moreland@auckland.ac.nz

Highlights

Total IgG3 is significantly elevated in acute rheumatic fever when compared to controls

Acute rheumatic fever displays an inflammatory triad comprising IL-6, CRP, and C4

Antibody responses polarize to IgG3 for M-protein and IgG1 for conserved GAS antigens

GAS-specific antibody responses are exaggerated in acute rheumatic fever

Article

An acute rheumatic fever immune signature comprising inflammatory markers, IgG3, and *Streptococcus pyogenes*-specific antibodies

Natalie Lorenz,[1,2,7] Reuben McGregor,[1,2,7] Alana L. Whitcombe,[1,2] Prachi Sharma,[1] Ciara Ramiah,[1] Francis Middleton,[1,2] Michael G. Baker,[2,3] William J. Martin,[4] Nigel J. Wilson,[5] Amy W. Chung,[6] and Nicole J. Moreland[1,2,8,*]

SUMMARY

Understanding the immune profile of acute rheumatic fever (ARF), a serious post-infectious sequelae of *Streptococcal pyogenes* (group A *Streptococcus* [GAS]), could inform disease pathogenesis and management. Circulating cytokines, immunoglobulins, and complement were analyzed in participants with first-episode ARF, swab-positive GAS pharyngitis and matched healthy controls. A striking elevation of total IgG3 was observed in ARF (90% > clinical reference range for normal). ARF was also associated with an inflammatory triad with significant correlations between interleukin-6, C-reactive protein, and complement C4 absent in controls. Quantification of GAS-specific antibody responses revealed that subclass polarization was remarkably consistent across the disease spectrum; conserved protein antigens polarized to IgG1, while M-protein responses polarized to IgG3 in all groups. However, the magnitude of responses was significantly higher in ARF. Taken together, these findings emphasize the association of exaggerated GAS antibody responses, IgG3, and inflammatory cytokines in ARF and suggest IgG3 testing could beneficially augment clinical diagnosis.

INTRODUCTION

Acute rheumatic fever (ARF) is a serious post-infectious, autoinflammatory consequence of a *Streptococcal pyogenes* (group A *Streptococcus* [GAS]) infection that can lead to permanent heart valve damage and rheumatic heart disease (RHD).[1] It is estimated that approximately 40 million people are living with RHD globally, with the highest disease burden in low and middle income countries.[2] The incidence of ARF and RHD remains unacceptably high among Indigenous populations in Australia and Māori and Pacific Peoples in Aotearoa New Zealand.[3,4]

The mechanisms by which a GAS infection triggers ARF are not completely understood. Molecular mimicry has been the prevailing hypothesis for many decades. The premise is that host proteins with similar coiled-coil structures to the GAS M-protein, such as cardiac myosin, are targeted by cross-reactive antibodies and T cells.[5] More recently, GAS infection has been proposed to expose cryptic collagen epitopes that initiate autoreactivity,[6] with collagen-reactive antibodies and T cells observed in patients with ARF and RHD.[7–9] However, profiling ARF autoantibodies with high-content protein arrays has revealed marked heterogeneity in the ARF autoantibody profile,[9] suggesting there is still much to be learned about the contribution of autoantibodies to pathogenesis.

There is now both serological and epidemiological data to suggest that repeated GAS infections are needed to prime the immune system and break tolerance for ARF to develop.[10–12] While GAS throat infections are a known precursor for ARF, there is increasing evidence that GAS skin infections might also be a trigger for ARF, either directly or as part of immune priming.[13,14] Priming via repeated GAS infections likely contributes to harmful, infection-driven inflammation. Inflammatory markers and cytokines have been observed in ARF, particularly C-reactive protein (CRP), interleukin-6 (IL-6), and tumor necrosis factor alpha (TNF-α), which are thought to promote inflammatory mediated tissue damage and disease symptoms.[15–17]

Though antibodies were observed infiltrating rheumatic heart valves in images taken some 60 years ago,[18] little is known about the contribution of immunoglobulin subclasses to infection responses in the context of immune priming and ARF pathogenesis. Of the four

[1]School of Medical Science, Faculty of Medical and Health Sciences, The University of Auckland, Auckland, New Zealand
[2]Maurice Wilkins Centre for Biodiscovery, The University of Auckland, Auckland, New Zealand
[3]Department of Public Health, University of Otago, Wellington, New Zealand
[4]Independent Advisor, Wellington, New Zealand
[5]Starship Children's Hospital, Health New Zealand – Te Whatu Ora, Auckland, New Zealand
[6]Department of Microbiology and Immunology, Peter Doherty Institute for Infection and Immunity, University of Melbourne, Melbourne, VIC, Australia
[7]These authors contributed equally
[8]Lead contact
*Correspondence: n.moreland@auckland.ac.nz
https://doi.org/10.1016/j.isci.2024.110558

Table 1. Demographic characteristics of study participants

	ARF (*n* = 60)	GAS (*n* = 30)	Healthy (*n* = 30)
Age, median (IQ range)	11 (9–13)	9 (7–11)	11.5 (9–13)
Sex,			
Male, n (%)	39 (65%)	17 (57%)	16 (53%)
Female, n (%)	21 (35%)	13 (43%)	14 (47%)
Ethnicity (prioritized)			
Māori, n (%)	17 (28%)	14 (47%)	10 (33%)
Pacific, n (%)	43 (72%)	16 (53%)	20 (67%)

immunoglobulin G (IgG) subclasses, IgG3 is the most potent in terms of affinity for complement factor protein C1q and Fcγ receptors, which, in turn, promote complement activation and antibody-mediated effector functions such as phagocytosis and cellular-mediated cytotoxicity.[19] Thus, while IgG3 only comprises approximately 5% of the total IgG in sera, it has an important role in the immune response to infections. However, over-production can be detrimental and excessive IgG3 has been associated with harmful inflammatory responses following infections[19,20] and in autoimmune diseases.[21,22]

We recently showed that serum IgG3 levels were significantly elevated in ARF patients compared with matched healthy controls, suggesting a role for IgG3 in ARF pathogenesis.[23] However, many questions remain as to the IgG3-related (and broader) immune features associated with precursor GAS infections and progression to ARF. Such features have potential as immune markers that could improve ARF diagnosis or inform new treatment strategies, with specific diagnostic tests and therapies that can stop cardiac damage completely lacking for this neglected disease.[24] Consequently, the aim of this study was to interrogate the immune profile in ARF to identify disease-associated signatures. Circulating immune molecules including IgG3, complement, and cytokines were analyzed in children with ARF, GAS pharyngitis and matched healthy controls recruited in New Zealand-based case-control studies.[25,26] Pathogen-specific antibody responses were assessed and systems immunology data analysis approaches were applied to identify relationships between key immune molecules that distinguish ARF from controls.

RESULTS

IgG3 and an inflammatory triad distinguish ARF from controls

To compare the systemic immune environment in uncomplicated GAS infections and ARF, the concentration of 25 circulating immune molecules was determined. This included 20 cytokines selected for relevance to ARF pathogenesis,[15] the four features we identified as distinguishing ARF from matched healthy controls in our prior, smaller-scale study (IgG1, IgG3, IgA, and complement C4),[23] as well as CRP—an inflammatory marker routinely used as part of the Jones criteria to diagnose ARF.[27] Participants comprised 60 children with first-episode ARF, 30 children with GAS-positive pharyngitis, and 30 closely matched healthy children (Table 1; Figure S1). Sera was obtained from ARF patients at a single time point during hospitalization, and the acute sample obtained from children with GAS-positive pharyngitis was utilized to compare inflammatory responses during GAS infection.

To initially assess the discriminative power of all 25 features, a partial least squares discriminant analysis (PLS-DA) was employed. A clear, though incomplete segregation of ARF patients was achieved, with the largest separation observed across latent-variable-1 (LV-1) (Figure 1A). The features driving the separation of ARF in LV-1 highlight a distinct immuno-inflammatory profile in comparison with GAS-pharyngitis and healthy controls with the top five features being IgG3, C4, IgG1, CRP, and IgA, followed by cytokines IL-6, IL-7, and A proliferation-inducing ligand (APRIL) (Figure 1B). Univariate analysis of all analytes between ARF and the GAS pharyngitis and healthy groups showed that only IgG3 was significantly elevated (*p* < 0.01) with a fold change (FC) >2 in both comparisons, while IL-6 and CRP were elevated 2-fold in ARF compared with the healthy group (Figure 1C). Correlation analysis of all significantly elevated features (*p* < 0.01) showed that the inflammatory triad of IL-6, CRP, and C4 was strongly correlated in ARF, but not in the other groups (Figure 1D). Interestingly, all cytokines that showed significant differences (*p* < 0.01) were highest in ARF, except for IP10, which was elevated in the GAS pharyngitis group (Figure 1E). This suggests a role for IP10 in the early infection response in line with findings from immunological analysis of the GAS human challenge model.[28] To explore the link between the circulating cytokines and their corresponding production from immune cells in ARF, cytokines secreted by peripheral blood mononuclear cells (PBMCs) obtained from a distinct, small cohort of ARF patients (*n* = 3) and healthy controls (*n* = 3) were quantified (Figure S3). Though based on low numbers, increased production of the four cytokines measured was evident from ARF PBMCs compared to healthy controls, all of which were also elevated in the large-scale serum analysis (Figure 1E; Figure S2).

Taken together, these results indicate a distinct immuno-inflammatory profile in ARF compared to GAS pharyngitis and healthy controls, characterized by elevated inflammatory cytokines, complement C4 and immunoglobulins, particularly IgG3. Indeed, IgG3 showed a striking elevation in ARF with levels above the upper limit of clinical reference ranges in 55/60 cases (Figure 2A), thereby validating our previous findings[23] with this extended cohort. The ability of IgG3 to distinguish ARF from a combined non-ARF control group (GAS pharyngitis and healthy) was assessed using a receiver operator curve (ROC) (Figure 2B). The area under the curve (AUC) showed IgG3 had very good predictive performance in this context (AUC = 0.93, confidence interval (CI):0.88–0.98).
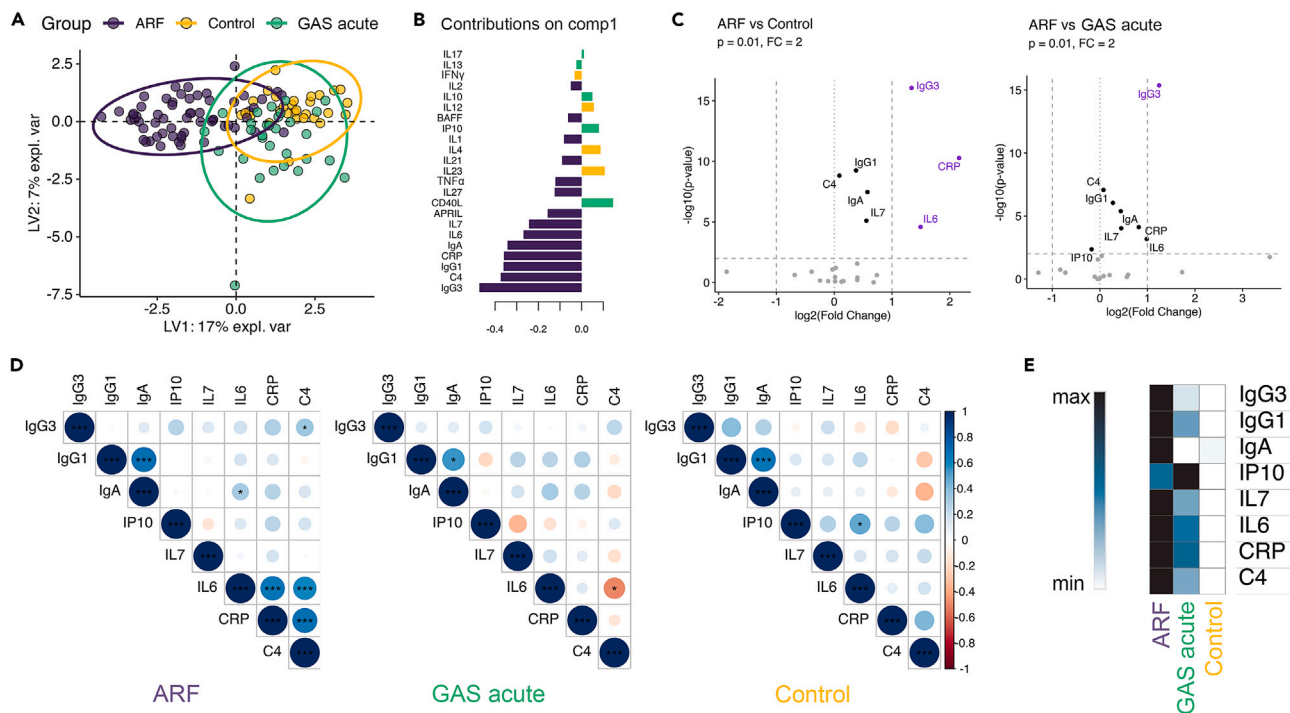
Figure 1. Differential immune profiling reveals IgG3 as a principal circulating marker distinguishing ARF from GAS pharyngitis and healthy controls

(A) PLS-DA analysis showing the separation of samples based on their immune profiles. The first latent variable (LV1) and second latent variable (LV2). Features displaying 0 variance were excluded (GM-CSF and TNFβ). Cross validation yielded a balanced error rate (BER) of 32%, showing no significant overfitting.

(B) Bar chart displaying the contributions of individual immune markers to the first component (comp1) in the PLS-DA analysis shown in (A). Contribution bar's colored by the group with the highest mean value in the raw data.

(C) Volcano plots showing the statistical significance (*p* value, horizontal dashed lines) versus fold change (vertical dashed lines) in concentrations of various immune markers. Purple dots and annotations highlight markers meeting both the significance and fold change thresholds (FDR adjusted *p* value <0.01, and fold change > 2, respectively), black dots represent immune markers meeting the significance threshold only.

(D) Correlation matrixes for study groups using Pearson correlations of log10 transformed concentration data (positive blue, negative red), with significant correlations as indicated (*, ***).

(E) Heatmap showing the *Z* score normalized median concentrations of immune markers identified as significant in the volcano plot analysis 1C.

GAS-specific antibody subclass polarization is consistent across the disease spectrum

To investigate the antigenic basis of the significant IgG3 elevation in ARF, alongside the broader GAS antibody response, a combination of multiplex bead-based assays and ELISA were performed. Initial investigations utilized our previously developed 8-plex assay encompassing conserved putative GAS vaccine antigens (Spy0843, streptococcal C5a peptidase [SCPA], *S. pyogenes* cell envelope protease [SpyCEP], *S. pyogenes* adhesion and division protein [SpyAD], group A carbohydrate [GAC], streptolysin O [SLO], DNaseB, and *S. pyogenes* nuclease A [SpnA]).[29,30] This 8-plex assay, originally designed for detection of total IgG, was expanded to enable detection of all relevant isotypes (IgG, IgA, and IgM) and IgG-subclasses (IgG1–4). To ensure complete seroconversion of antibody responses, convalescent sera from the GAS pharyngitis cases obtained approximately 1 month following infection were also analyzed.

Total IgG concentration for all eight antigens was significantly elevated in ARF compared to GAS pharyngitis (acute and convalescent) and matched healthy controls, replicating our prior findings[30] (Figure 3A). Similar patterns were observed for IgA, with significant increases in ARF compared with matched healthy controls for all eight antigens, and for five of the antigens (Spy0843, SCPA, SpyCEP, SpyAD, and GAC) when compared with GAS pharyngitis (Figure 3A). Fewer antigens showed significant IgM elevation in ARF compared with matched healthy controls and GAS pharyngitis, and as would be expected in response to a polysaccharide antigen,[31] anti-GAC IgM was generally elevated in all groups (Figure 3A).

IgG subclass analysis showed that all four subclasses were significantly elevated against the 8-plex antigens in ARF compared to matched healthy controls with very few exceptions. However, significant differences between ARF and GAS pharyngitis were less consistent—while IgG1 and IgG2 were significantly elevated for all antigens, this was observed for fewer antigens with IgG3 (SCPA, SpyCEP, SpyAD, and DNaseB) and only one antigen with IgG4 (SpnA) (Figure S4). Interestingly, a comparison of subclass distribution for each antigen showed that IgG1 tended to dominate the response regardless of disease group (Figure 3B). The exception being the GAC, which showed an IgG2 dominance, in line with IgG2 being the principal subclass response to bacterial polysaccharides.[32] IgG4
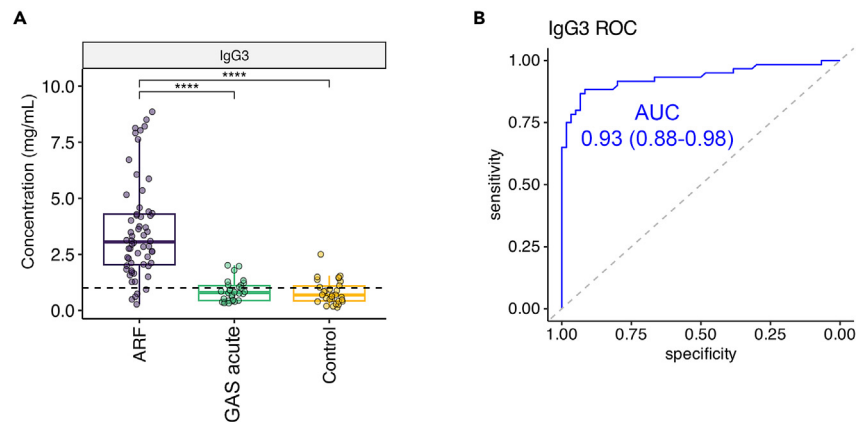
Figure 2. Striking elevation in IgG3 concentrations in ARF

(A) Boxplots illustrating the distribution of IgG3 concentrations across study groups. The upper limit of the clinical reference range is shown as dashed horizontal line. In boxplot the middle line represents the median. The lower and upper hinges correspond to the 25th and 75th percentiles, with upper and lower whiskers extending to the highest and lowest values, respectively. but no further than 1.5× the interquartile range.

(B) A receiver operator curve (ROC) curve comparing ARF to all controls. Gray dashed line represents the line of no discrimination and the area under the curve (AUC) with confidence interval as indicated. The confidence interval was obtained using bootstrapping, $n = 2,000$.

responses were generally low in comparison with other subclasses. Of note, IgG3 did not dominate responses to the 8-plex antigens or the responses in the ARF group (Figure 3B), suggesting the elevated IgG3 observed in ARF is not driven by the conserved, GAS vaccine antigens examined.

To further interrogate the antigen specificity of IgG3, responses to M-protein antigens were assessed using ELISA. Our prior study, based on a limited number of ARF patients and a single M-protein antigen, suggested IgG3 polarization to M-proteins.[23] Here two full-length M-proteins were included, one derived from a strain historically termed "rheumatogenic" (M6) and the second from a strain contemporarily associated with ARF in our setting (M53).[33,34] A further construct containing the M-protein C2-C3 repeat region, highly conserved between M-types, was also designed and included (designated M_C2_C3). SLO was utilized as a control conserved antigen to bridge the two immunoassay approaches, and total IgG to SLO was highly correlated between the 8-plex and ELISA (Figure S5C). Consistent with the increased magnitude of anti-GAS antibodies observed in ARF with the 8-plex assay, the ARF group showed significantly increased total IgG, as well as IgG1 and IgG3, to all three M-protein antigens compared to GAS pharyngitis and healthy children (Figure 4A; Figure S5A). When subclass responses were compared for each antigen, a marked and significant skewing of IgG3 responses for M-proteins and M_C2_C3 was observed in all disease groups. This pattern was reversed for the conserved SLO antigen, with IgG1 dominating the response (Figure 4B). When total IgG responses were correlated to Ig-subclasses in the ARF group, strong correlations were seen between total IgG (IgG$_{tot}$) and IgG3 for all three M-protein-based antigens (r > 0.9), but not for IgG1. Again this pattern was reversed for SLO, where there was a strong correlation between IgG$_{tot}$ and IgG1 but not for IgG3 (Figure 4C). These data suggest that the elevated IgG3 observed in ARF may, in part, be driven by IgG3 polarized responses to M-protein antigens, rather than conserved antigens such as SLO. Furthermore, the M-protein IgG3 responses in ARF were strongly correlated between each of the three antigens (M6, M53, and M_C2_C3), indicating that much of the observed anti-M IgG3 reacts with conserved regions of the M protein (Figure S5B).

Network analysis reinforces inflammation and exaggerated anti-M IgG3 responses in ARF

To gain a global overview of interactions between all the immune features measured, a correlation network was constructed between all analytes for the ARF sera group that showed significant relationships in a multiple comparison analyses as defined (r > 0.6 and $p < 0.05$) (Figure 5). As expected, the observed C4-CRP-IL6 inflammatory triad was correlated in this wider analysis, and the IgG1 responses to conserved antigens correlated strongly with the IgG$_{tot}$ response for the same antigen. The exception being GAC where IgG$_{tot}$ correlated with IgG2. IgM responses to five conserved antigens formed a correlated cluster (SpyCEP, Spy0843, DNaseB, SpyAD, and SLO), suggesting possible relationships in early anti-GAS responses. IgG1 responses to all three M-protein targets also formed a separate correlated cluster, though this was not linked to IgG$_{tot}$ responses for M-protein antigens. Rather, the biggest cluster was formed between IgG$_{tot}$ and IgG3 responses to all three M-protein targets, with strong correlations throughout. This large cluster was linked via weaker correlations to IgG3 responses to SpnA and DNaseB. However, much stronger correlations were observed for IgG$_{tot}$ and IgG1 responses for these two conserved antigens. This global view reinforces the inflammatory nature of ARF (C4-CRP-IL-6) as well as highly correlated, but seemingly distinct subclass skewing to conserved antigens (IgG1 skewed) compared with M-protein based antigens (IgG3 skewed). Intriguingly, total IgG3 was not observed in this analysis, as while it was moderately correlated with some features, these relationships did not meet the threshold for inclusion. This finding suggests that the biological basis for the significant elevation of IgG3 in ARF is complex and not fully explained by the immune features included in this study.
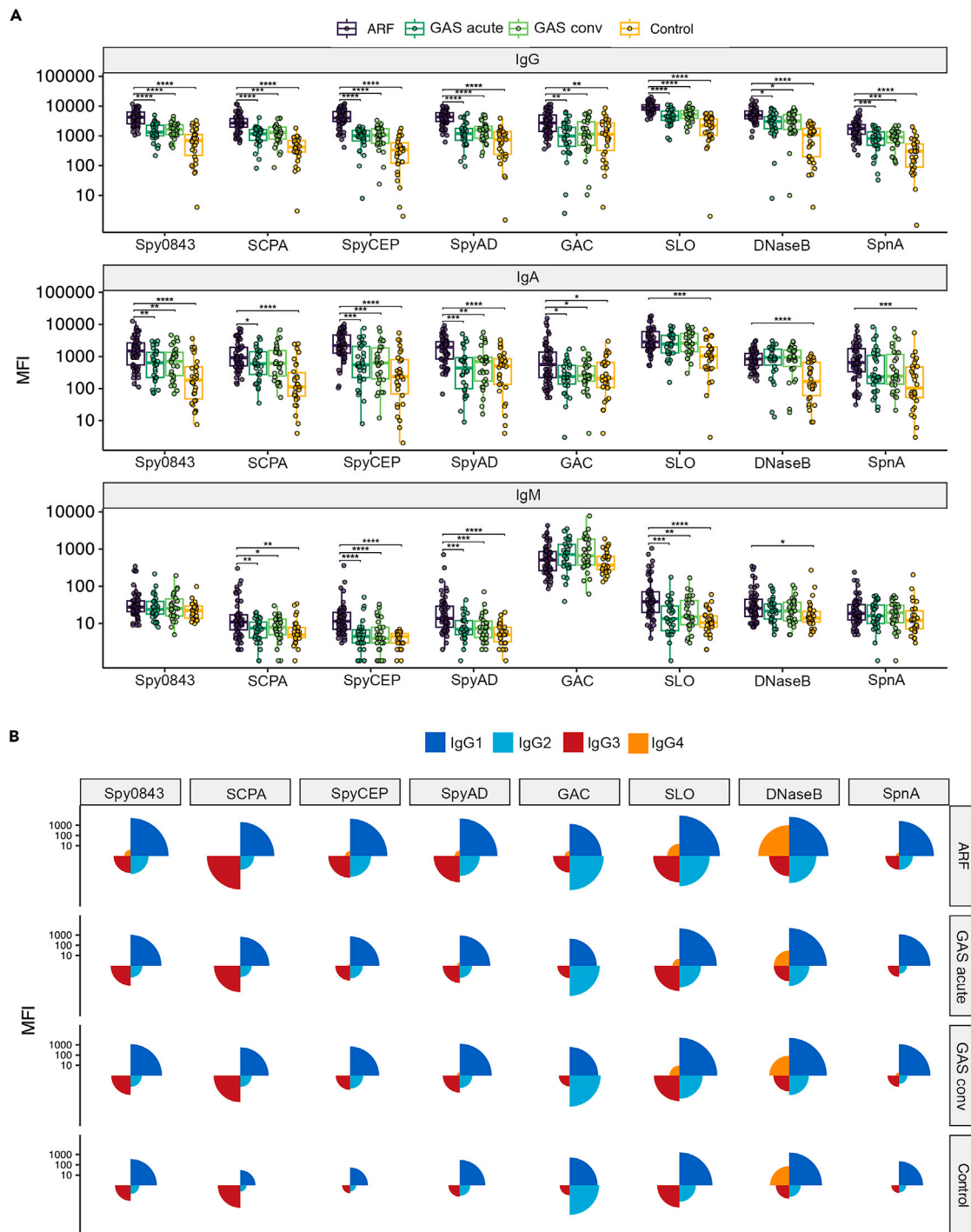
Figure 3. Antibody isotypes and IgG subclasses in acute rheumatic fever

(A) Boxplots depicting the MFI of IgG, IgA, and IgM antibodies across the 8-plex antigens in the different study groups. In boxplots the middle line represents the median. The lower and upper hinges correspond to the 25th and 75th percentiles, with upper and lower whiskers extending to the highest and lowest values, respectively, but no further than 1.5× the interquartile range.

(B) Rose plots visualizing the IgG subclass response (IgG1, IgG2, IgG3, and IgG4) to the 8-plex antigens across the study groups using the median MFI. GAS conv, GAS convalescent.
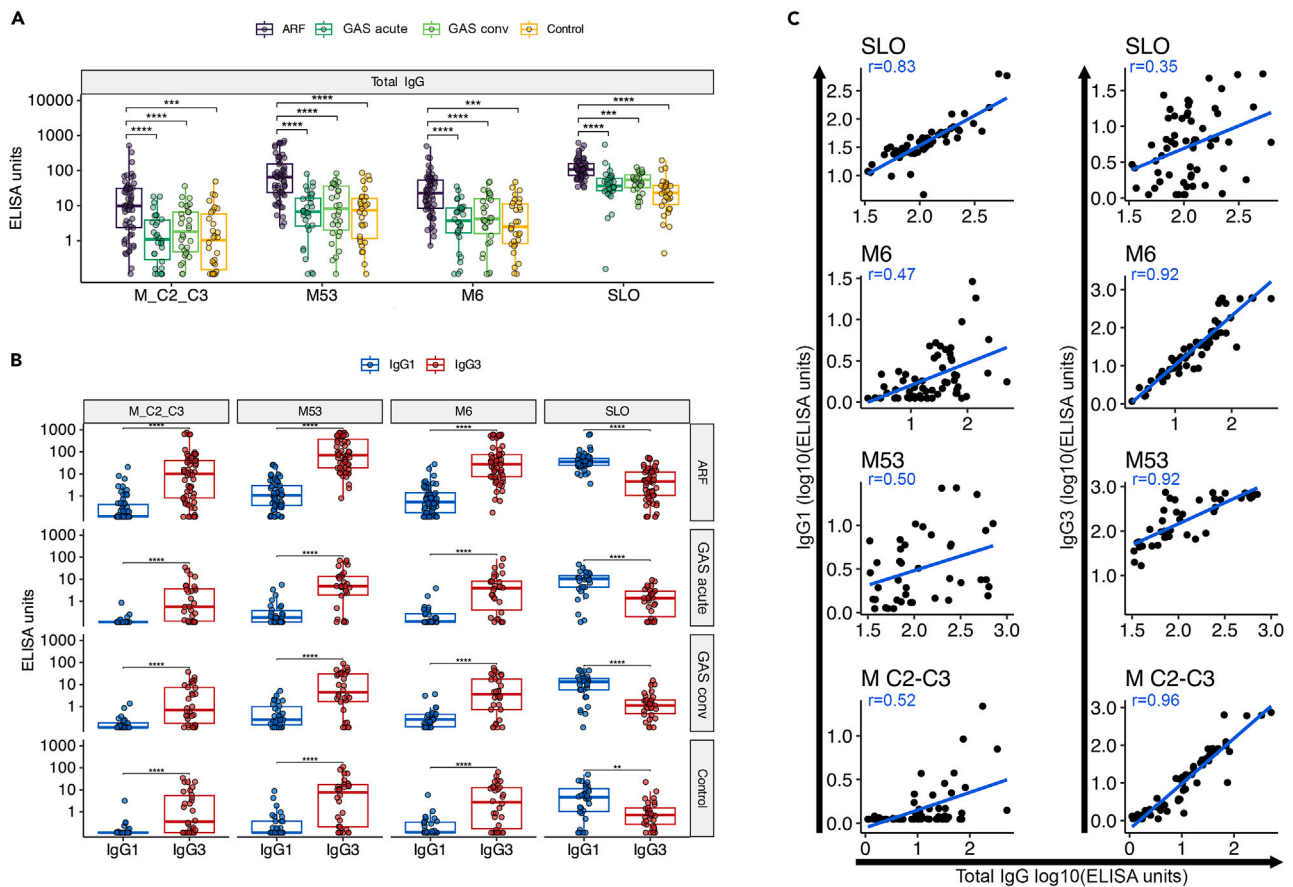
Figure 4. IgG3 polarization to M-protein

(A) Boxplots depicting total IgG as ELISA units to M protein antigens (M6, M53 and M_C2_C3) and conserved antigen SLO in the different study groups. GAS conv, GAS convalescent.

(B) Boxplots depicting in ELISA units, total IgG1 and IgG3 subclass responses to the same antigens as (a) across the three study groups.

(C) IgG1 (left) and IgG3 (right) correlations with total IgG in ARF cases across the M-protein and SLO antigens. Pearson's correlations of log10 transformed data were used with correlations (r) as shown.

In boxplots the middle line represents the median. The lower and upper hinges correspond to the 25th and 75th percentiles, with upper and lower whiskers extending to the highest and lowest values, respectively, but no further than 1.5× the interquartile range.

DISCUSSION

This study illustrates the striking elevation of circulating IgG3 in children with first-episode ARF, extending on our prior observations.[23] Over 90% of ARF children in this study had IgG3 levels above the clinical reference range of normal, and the ROC analysis suggests that IgG3 testing has the potential to augment diagnosis. The diagnosis of ARF currently relies on country-specific adaptations of the Jones criteria,[35] and improved tests are needed to address the large diagnostic gaps observed. In many settings globally, first episode ARF is often missed such that up to 80% of RHD diagnoses are made in the absence of a prior ARF diagnosis.[36,37] In our New Zealand setting this diagnosis gap is reduced, but still notable with 41% of RHD presentations occurring without a prior ARF diagnosis in a recent audit of nearly 5,000 patients.[38] Clinical tests for serum IgG3 are already available and used routinely for the diagnosis of immunodeficiencies,[39] raising the possibility of larger studies to evaluate IgG3-augmentation for ARF diagnosis. While IgG3 is not specific for ARF, as it is elevated in other immune-mediated diseases,[19,22] it could improve the performance of the Jones criteria by identifying false negatives (missed cases).

The role of IgG3 in ARF pathogenesis may be linked to the inflammatory nature of the disease. The observation of elevated IL-6, complement C4 and CRP points clearly to the inflammation underlying ARF, in keeping with earlier studies.[15,16,23,40] IgG3 is also elevated in patients with other autoimmune and immune-mediated conditions such as multiple sclerosis (MS) and human immune deficiency virus (HIV). In MS, elevated IgG3 in sera and IgG3+ B cell subsets are associated with conversion to disease and autoimmune attack on the central nervous system.[21,41] In HIV-infected individuals, elevated IgG3 has been linked with chronic antigen stimulation,[42] with this proposed to bind and negatively regulate tissue-like memory B cells in those with chronic infections.[43] Elevated serum IgG3
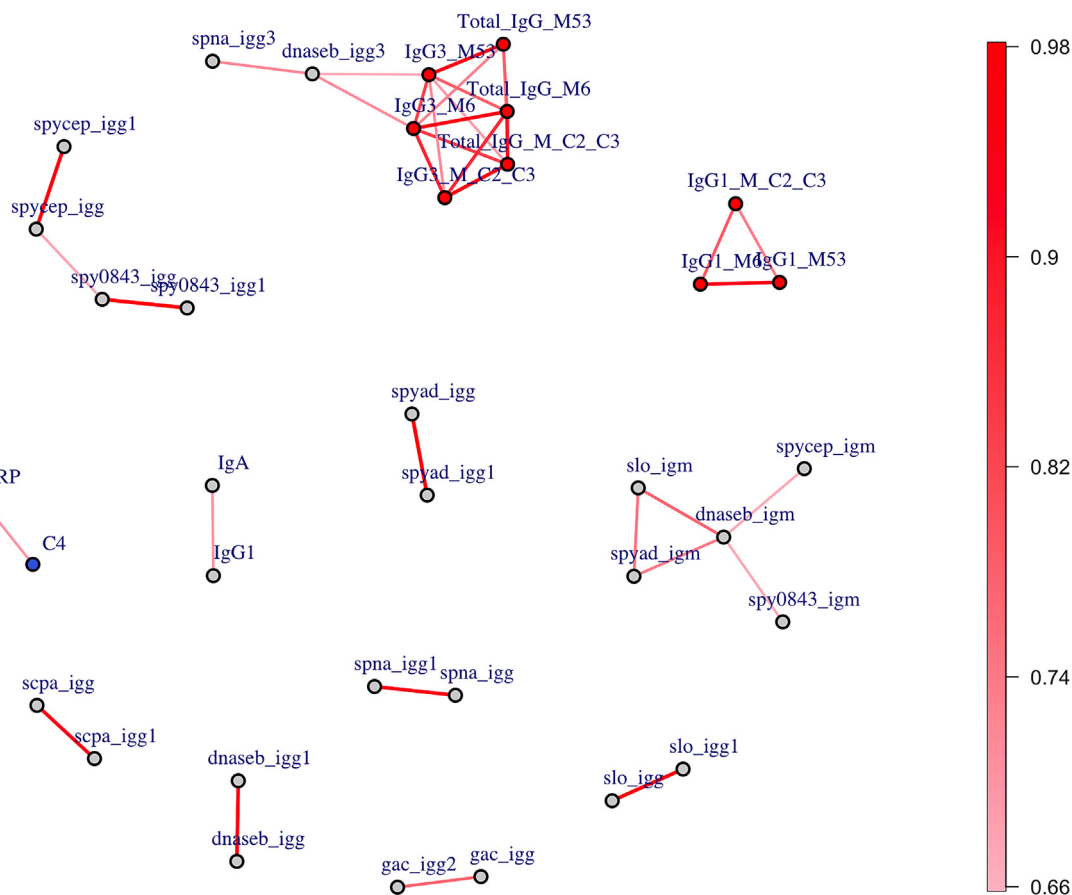
Figure 5. Network correlation plot of combined data in ARF cases

A correlation network plot of immune markers and GAS antibody responses measured using an 8-plex Luminex assay and an M-protein-specific ELISA. Only markers that showed significant elevation in ARF were retained. Nodes in the network represent individual markers from the combined datasets and edges between nodes correspond to significant correlations, with edge thickness and color proportional to the absolute value of the Pearson correlation coefficient as indicated by scale (right). The nodes are colored by type of marker with light blue = cytokines, dark blue = other circulating inflammatory markers, red = M-protein markers and gray = 8-plex Luminex data. Only significant ($p < 0.05$ after Holm-Bonferroni adjustment) strong correlations (absolute Pearson's correlation coefficient > 0.6) were retained.

may also be a marker of chronic immune activation in ARF and gaining mechanistic insight of the immune cells producing IgG3 in ARF, and the links between these mechanisms and inflammation may provide an avenue for therapeutic intervention. There is a complete lack of therapies that can stop progression of ARF to RHD, despite the range of treatments available for other pediatric autoinflammatory conditions.[15] Studies of low-dose hydroxychloroquine, a general anti-inflammatory agent, are now underway in New Zealand.[44] The clear elevation of IL-6 observed in this study suggests IL-6 blockade therapies like tocilizumab are also worth consideration, particularly since tocilizumab has been shown to reduce serum IgG3 levels clinically.[45]

The profile of isotype and subclass responses to GAS antigens in this study offers insight into pathogen specific Ig-responses across the spectrum of disease. Antigen-specific patterns of subclass polarization were remarkably consistent between disease states, with the most notable differences being the higher magnitude of responses in ARF. As expected for a bacterial polysaccharide, IgG2 dominated responses to GAC irrespective of disease state. This finding is consistent with the IgG2 skewing observed to the N-acetyl-β-D-glucosamine (GlcNAc) side chain of GAC in children with GAS pharyngitis and RHD.[46] Interestingly for protein antigens, IgG1 dominated responses to conserved proteins, while IgG3 dominated responses to M-protein antigens. IgG3 dominance of M-protein responses was also recently demonstrated in pooled intravenous immunoglobulin (IVIG) using mass spectrometry, with M-protein knockout strains having significantly reduced IgG3 binding.[47] What drives such a marked difference in subclass polarization between protein antigens presented on the same pathogen is unclear. It is possible that the coiled-coil structure of the M-protein is preferentially recognized by IgG3 molecules due to the extended hinge flexibility, or other unique biophysical properties of this diverse subclass.[19] Immunoglobulin expression order may also play a role, with IgG3 generally expressed before IgG1.[48] The type-specific hyper-variable region would represent a new antigen in individuals infected with an M-type for the first time and may trigger early IgG3 responses following exposure.

M-protein antigens are known to induce opsonization and killing of GAS, and M-protein based vaccine candidates are in various stages of development.[49] Given the potent activity of IgG3 with respect to Fc receptor engagement and phagocytosis,[19] it is probable that IgG3 binding to M-proteins contributes to protective immune responses induced by M-protein antigens. Indeed, phagocytosis studies with an M5 GAS strain linked IgG3 binding of M-proteins with complement activation and bacterial internalization.[47] However, there will likely be a need for M-protein based vaccine candidates to balance these protective IgG3-driven responses and avoid over-stimulation and the potentially harmful, inflammatory effects of IgG3. The repeated exposures of GAS that are proposed to lead to a loss of tolerance in ARF via immune priming,[10–12] may drive the exaggerated IgG3 responses to M-proteins observed in ARF. This pathogen-driven IgG3 response could, in turn, contribute to immune dysregulation. Similar phenomena are proposed in severe dengue and active tuberculosis where over-induction of IgG3 effector functions has been linked with excessive inflammatory responses and serious disease.[19]

Beyond the link between GAS M-proteins and antigen-specific IgG3 responses, the lack of any strong correlation between total IgG3 and other immune features in this study suggests there is still much to learn with respect to IgG3 in ARF. A recent study has shown that M-related proteins (Mrp), which are expressed in the same regulon as M-proteins, have significantly reduced affinity for IgG3,[50] and it is possible that Mrp protein responses influence M-protein responses in ARF. IgG3-driven autoantibody responses may also contribute to the elevated levels of IgG3 observed. While total IgG levels to autoantigens have been shown to be elevated in ARF, subclass responses have not been widely reported.[9,51] Similarly, the role of T cell activation in isotype switching to IgG3 is yet to be explored in ARF and may contribute to the significantly elevated IgG3 levels observed.

In conclusion, this study observed exaggerated GAS-specific antibody responses, elevated total IgG3 and inflammatory cytokines in ARF. These features may contribute to a permissive inflammatory environment that leads to the immune-mediated tissue damage observed in symptomatic disease. Furthermore, measurement of serum IgG3 levels may beneficially augment clinical algorithms for ARF diagnosis.

Limitations of the study

This study comprises samples from participants recruited in two aligned, but not concurrent, case-control studies. The first recruited first-episode ARF cases and closely matched controls between 2014 and 2017,[25] while the second recruited participants with GAS-positive pharyngitis between 2018 and 2019.[26] Matching in the first study was by age, ethnicity, socioeconomic deprivation, and region followed by sex, explaining the slight sex imbalance in ARF cases compared with healthy controls in this study cohort. The second study investigated GAS infections in school-aged children in Auckland, New Zealand. While not temporally matched with the ARF cases, GAS-positive pharyngitis participants included in this study cohort were assessed using the same risk-factors questionnaire and closely matched for age and ethnicity.

STAR★METHODS

Detailed methods are provided in the online version of this paper and include the following:

- KEY RESOURCES TABLE
- RESOURCE AVAILABILITY
  - Lead contact
  - Materials availability
  - Data and code availability
- EXPERIMENTAL MODEL AND STUDY PARTICIPANT DETAILS
- METHOD DETAILS
  - Circulating analyte quantification
  - Primary cell culture assays
  - Group A Streptococcus Luminex assays
  - Group A Streptococcus ELISA
- QUANTIFICATION AND STATISTICAL ANALYSIS

SUPPLEMENTAL INFORMATION

Supplemental information can be found online at https://doi.org/10.1016/j.isci.2024.110558.

AUTHOR CONTRIBUTIONS

N.L., R.M., A.L.W., A.W.C., and N.J.M. initiated and designed the study. N.L., A.L.W., P.S., C.R., and F.M. performed experiments and N.L., R.M., and A.L.W. analyzed the results. R.M., M.G.B., W.J.M., N.J.W., A.W.C., and N.J.M. obtained funding and together with N.L. interpreted the results. N.L., R.M., and N.J.M. co-wrote the original manuscript, and all authors read and reviewed the manuscript.

DECLARATION OF INTERESTS

N.J.M. is a co-inventor on a patent related to rheumatic fever diagnostics (PCT/NZ2018/050057).

REFERENCES

1. Walker, M.J., Barnett, T.C., McArthur, J.D., Cole, J.N., Gillen, C.M., Henningham, A., Sriprakash, K.S., Sanderson-Smith, M.L., and Nizet, V. (2014). Disease manifestations and pathogenic mechanisms of group a Streptococcus. Clin. Microbiol. Rev. 27, 264–301. https://doi.org/10.1128/cmr.00101-13.

2. Beaton, A., Kamalembo, F.B., Dale, J., Kado, J.H., Karthikeyan, G., Kazi, D.S., Longenecker, C.T., Mwangi, J., Okello, E., Ribeiro, A.L.P., et al. (2020). The American Heart Association's Call to Action for Reducing the Global Burden of Rheumatic Heart Disease: A Policy Statement From the American Heart Association. Circulation 142, e358–e368. https://doi.org/10.1161/cir.0000000000000922.

3. Bennett, J., Zhang, J., Leung, W., Jack, S., Oliver, J., Webb, R., Wilson, N., Sika-Paotonu, D., Harwood, M., and Baker, M.G. (2021). Rising Ethnic Inequalities in Acute Rheumatic Fever and Rheumatic Heart Disease, New Zealand, 2000-2018. Emerg. Infect. Dis. 27, 36–46. https://doi.org/10.3201/eid2701.191791.

4. Egoroff, N., Bloomfield, H., Gondarra, W., Yambalpal, B., Guyula, T., Forward, D., Lyons, G., O'Connor, E., Sanderson, L., Dowden, M., et al. (2023). An outbreak of acute rheumatic fever in a remote Aboriginal community. Aust. N. Z. J. Publ. Health 47, 100077. https://doi.org/10.1016/j.anzjph.2023.100077.

5. Carapetis, J.R., Beaton, A., Cunningham, M.W., Guilherme, L., Karthikeyan, G., Mayosi, B.M., Sable, C., Steer, A., Wilson, N., Wyber, R., and Zühlke, L. (2016). Acute rheumatic fever and rheumatic heart disease. Nat. Rev. Dis. Primers 2, 15084. https://doi.org/10.1038/nrdp.2015.84.

6. Tandon, R., Sharma, M., Chandrashekhar, Y., Kotb, M., Yacoub, M.H., and Narula, J. (2013). Revisiting the pathogenesis of rheumatic fever and carditis. Nat. Rev. Cardiol. 10, 171–177. https://doi.org/10.1038/nrcardio.2012.197.

7. Pilapitiya, D.H., Harris, P.W.R., Hanson-Manful, P., McGregor, R., Kowalczyk, R., Raynes, J.M., Carlton, L.H., Dobson, R.C.J., Baker, M.G., Brimble, M., et al. (2021). Antibody responses to collagen peptides and streptococcal collagen-like 1 proteins in acute rheumatic fever patients. Pathog. Dis. 79, ftab033. https://doi.org/10.1093/femspd/ftab033.

8. Passos, L.S.A., Jha, P.K., Becker-Greene, D., Blaser, M.C., Romero, D., Lupieri, A., Sukhova, G.K., Libby, P., Singh, S.A., Dutra, W.O., et al. (2022). Prothymosin Alpha: A Novel Contributor to Estradiol Receptor Alpha–Mediated CD8 + T-Cell Pathogenic Responses and Recognition of Type 1 Collagen in Rheumatic Heart Valve Disease. Circulation 145, 531–548. https://doi.org/10.1161/circulationaha.121.057301.

9. McGregor, R., Tay, M.L., Carlton, L.H., Hanson-Manful, P., Raynes, J.M., Forsyth, W.O., Brewster, D.T., Middleditch, M.J., Bennett, J., Martin, W.J., et al. (2021). Mapping Autoantibodies in Children With Acute Rheumatic Fever. Front. Immunol. 12, 702877. https://doi.org/10.3389/fimmu.2021.702877/full.

10. Lorenz, N., Ho, T.K.C., McGregor, R., Davies, M.R., Williamson, D.A., Gurney, J.K., Smeesters, P.R., Baker, M.G., and Moreland, N.J. (2021). Serological Profiling of Group A Streptococcus Infections in Acute Rheumatic Fever. Clin. Infect. Dis. 73, 2322–2325. https://doi.org/10.1093/cid/ciab180.

11. Zabriskie, J.B. (1967). Mimetic relationships between group A streptococci and mammalian tissues. Adv. Immunol. 7, 147–188. https://doi.org/10.1016/s0065-2776(08)60128-5.

12. Raynes, J.M., Frost, H.R.C., Williamson, D.A., Young, P.G., Baker, E.N., steemson, J.D., Loh, J.M., Proft, T., Dunbar, P.R., Atatoa Carr, P.E., et al. (2016). Serological Evidence of Immune Priming by Group A Streptococci in Patients with Acute Rheumatic Fever. Front. Microbiol. 7, 1119. https://doi.org/10.3389/fmicb.2016.01119.

13. Oliver, J., Bennett, J., Thomas, S., Zhang, J., Pierse, N., Moreland, N.J., Williamson, D.A., Jack, S., and Baker, M. (2021). Preceding group A streptococcus skin and throat infections are individually associated with acute rheumatic fever: evidence from New Zealand. BMJ Glob. Health 6, e007038. https://doi.org/10.1136/bmjgh-2021-007038.

14. McDonald, M., Currie, B.J., and Carapetis, J.R. (2004). Acute rheumatic fever: a chink in the chain that links the heart to the throat? Lancet Infect. Dis. 4, 240–245. https://doi.org/10.1016/s1473-3099(04)00975-2.

15. Middleton, F.M., McGregor, R., Webb, R.H., Wilson, N.J., and Moreland, N.J. (2022). Cytokine imbalance in acute rheumatic fever and rheumatic heart disease: Mechanisms and therapeutic implications. Autoimmun. Rev. 21, 103209. https://doi.org/10.1016/j.autrev.2022.103209.

16. Yeğin, O., Coşkun, M., and Ertuğ, H. (1997). Cytokines in acute rheumatic fever. Eur. J. Pediatr. 156, 25–29. https://doi.org/10.1007/s004310050545.

17. Kim, M.L., Martin, W.J., Minigo, G., Keeble, J.L., Garnham, A.L., Pacini, G., Smyth, G.K., Speed, T.P., Carapetis, J., and Wicks, I.P. (2018). Dysregulated IL-1β-GM-CSF Axis in Acute Rheumatic Fever That Is Limited by Hydroxychloroquine. Circulation 138, 2648–2661. https://doi.org/10.1161/circulationaha.118.033891.

18. Kaplan, M.H., Bolande, R., Rakita, L., and Blair, J. (1964). Presence of Bound Immunoglobulins and Complement in the Myocardium in Acute Rheumatic Fever — Association with Cardiac Failure. N. Engl. J. Med. 271, 637–645. https://doi.org/10.1056/nejm196409242711301.

19. Damelang, T., Rogerson, S.J., Kent, S.J., and Chung, A.W. (2019). Role of IgG3 in Infectious Diseases. Trends Immunol. 40, 197–211. https://doi.org/10.1016/j.it.2019.01.005.

20. de Araujo, L.S., da Silva, N.d.B.M., Leung, J.A.M., Mello, F.C.Q., and Saad, M.H.F. (2018). IgG subclasses' response to a set of mycobacterial antigens in different stages of Mycobacterium tuberculosis infection. Tuberculosis 108, 70–76. https://doi.org/10.1016/j.tube.2017.10.010.

21. Marsh-Wakefield, F., Ashhurst, T., Trend, S., McGuire, H.M., Juillard, P., Zinger, A., Jones, A.P., Kermode, A.G., Hawke, S., Grau, G.E., et al. (2020). IgG3 + B cells are associated with the development of multiple sclerosis. Clin.

Transl. Immunol. 9, e1133. https://doi.org/10.1002/cti2.1133.

22. Zhang, H., Li, P., Wu, D., Xu, D., Hou, Y., Wang, Q., Li, M., Li, Y., Zeng, X., Zhang, F., and Shi, Q. (2015). Serum IgG subclasses in autoimmune diseases. Medicine (Baltim.) 94, e387. https://doi.org/10.1097/md.0000000000000387.

23. Chung, A.W., Ho, T.K., Hanson-Manful, P., Tritscheller, S., Raynes, J.M., Whitcombe, A.L., Tay, M.L., McGregor, R., Lorenz, N., Oliver, J.R., et al. (2020). Systems immunology reveals a linked IgG3-C4 response in patients with acute rheumatic fever. Immunol. Cell Biol. 98, 12–21. https://doi.org/10.1111/imcb.12298.

24. Ralph, A.P., Webb, R., Moreland, N.J., McGregor, R., Bosco, A., Broadhurst, D., Lassmann, T., Barnett, T.C., Benothman, R., Yan, J., et al. (2021). Searching for a technology-driven acute rheumatic fever test: the START study protocol. BMJ Open 11, e053720. https://doi.org/10.1136/bmjopen-2021-053720.

25. Baker, M.G., Gurney, J., Moreland, N.J., Bennett, J., Oliver, J., Williamson, D.A., Pierse, N., Wilson, N., Merriman, T.R., Percival, T., et al. (2022). Risk factors for acute rheumatic fever: A case-control study. Lancet Reg. Health. West. Pac. 26, 100508. https://doi.org/10.1016/j.lanwpc.2022.100508.

26. Bennett, J., Moreland, N.J., Zhang, J., Crane, J., Sika-Paotonu, D., Carapetis, J., Williamson, D.A., and Baker, M.G. (2022). Risk factors for group A streptococcal pharyngitis and skin infections: A case control study. Lancet Reg. Health. West. Pac. 26, 100507. https://doi.org/10.1016/j.lanwpc.2022.100507.

27. Wilson, N.J., Voss, L., Morreau, J., Stewart, J., and Lennon, D. (2013). New Zealand guidelines for the diagnosis of acute rheumatic fever: small increase in the incidence of definite cases compared to the American Heart Association Jones criteria. N. Z. Med. J. 126, 50–59.

28. Anderson, J., Imran, S., Frost, H.R., Azzopardi, K.I., Jalali, S., Novakovic, B., Osowicki, J., Steer, A.C., Licciardi, P.V., and Pellicci, D.G. (2022). Immune signature of acute pharyngitis in a Streptococcus pyogenes human challenge trial. Nat. Commun. 13, 769. https://doi.org/10.1038/s41467-022-28335-3.

29. Whitcombe, A.L., Han, F., McAlister, S.M., Kirkham, L.-A.S., Young, P.G., Ritchie, S.R., Atatoa Carr, P., Proft, T., and Moreland, N.J. (2022). An eight-plex immunoassay for Group A streptococcus serology and vaccine development. J. Immunol. Methods 500, 113194. https://doi.org/10.1016/j.jim.2021.113194.

30. Whitcombe, A.L., McGregor, R., Bennett, J., Gurney, J.K., Williamson, D.A., Baker, M.G., and Moreland, N.J. (2022). Increased Breadth of Group A Streptococcus Antibody Responses in Children With Acute Rheumatic Fever Compared to Precursor Pharyngitis and Skin Infections. J. Infect. Dis. 226, 167–176. https://doi.org/10.1093/infdis/jiac043.

31. Kappler, K., and Hennet, T. (2020). Emergence and significance of carbohydrate-specific antibodies. Gene Immun. 21, 224–239. https://doi.org/10.1038/s41435-020-0105-9.

32. Hammarström, L., and Smith, C.I. (1983). IgG2 deficiency in a healthy blood donor. Concomitant lack of IgG2, IgA and IgE immunoglobulins and specific anti-carbohydrate antibodies. Clin. Exp. Immunol. 51, 600–604.

33. de Crombrugghe, G., Baroux, N., Botteaux, A., Moreland, N.J., Williamson, D.A., Steer, A.C., and Smeesters, P.R. (2020). The Limitations of the Rheumatogenic Concept for Group A Streptococcus: Systematic Review and Genetic Analysis. Clin. Infect. Dis. 70, 1453–1460. https://doi.org/10.1093/cid/ciz425.

34. Williamson, D.A., Smeesters, P.R., Steer, A.C., steemson, J.D., Ng, A.C.H., Proft, T., Fraser, J.D., Baker, M.G., Morgan, J., Carter, P.E., and Moreland, N.J. (2015). M-Protein Analysis of Streptococcus pyogenes Isolates Associated with Acute Rheumatic Fever in New Zealand. J. Clin. Microbiol. 53, 3618–3620. https://doi.org/10.1128/jcm.02129-15.

35. Osowicki, J., and Steer, A.C. (2020). Diagnosis of rheumatic fever: the need for a better test. Arch. Dis. Child. 105, 813–814. https://doi.org/10.1136/archdischild-2020-318970.

36. Ralph, A.P., and Carapetis, J.R. (2013). Group a streptococcal diseases and their global burden. Curr. Top. Microbiol. Immunol. 368, 1–27. https://doi.org/10.1007/82_2012_280.

37. Hempenstall, A., Howell, E., Kang, K., Chau, K.W.T., Browne, A., Kris, E., Wapau, H., Pilot, P., Smith, S., Reeves, B., and Hanson, J. (2021). Echocardiographic Screening Detects Rheumatic Heart Disease and Missed Opportunities in the Treatment of Group A Streptococcal Infections in Australian Torres Strait Islander Children. Am. J. Trop. Med. Hyg. 104, 1211–1214. https://doi.org/10.4269/ajtmh.20-0846.

38. Tilton, E., Mitchelson, B., Anderson, A., Peat, B., Jack, S., Lund, M., Webb, R., and Wilson, N. (2022). Cohort profile: methodology and cohort characteristics of the Aotearoa New Zealand Rheumatic Heart Disease Registry. BMJ Open 12, e066232. https://doi.org/10.1136/bmjopen-2022-066232.

39. Parker, A.R., Skold, M., Ramsden, D.B., Ocejo-Vinyals, J.G., López-Hoyos, M., and Harding, S. (2017). The Clinical Utility of Measuring IgG Subclass Immunoglobulins During Immunological Investigation for Suspected Primary Antibody Deficiencies. Lab. Med. 48, 314–325. https://doi.org/10.1093/labmed/lmx058.

40. Bhattacharya, S., Reddy, K.S., Sundaram, K.R., Chopra, P., Prakash, K., Malaviya, A.N., and Tandon, R. (1987). Differentiation of patients with rheumatic fever from those with inactive rheumatic heart disease using the artificial subcutaneous nodule test, myocardial reactive antibodies, serum immunoglobulin and serum complement levels. Int. J. Cardiol. 14, 71–78. https://doi.org/10.1016/0167-5273(87)90180-x.

41. Kennedy, P.G.E., Graner, M.W., Fringuello, A., Zhou, W., Pointon, T., Alquatli, K., Bisel, S., Langford, D., and Yu, X. (2022). Higher Levels of IgG3 Antibodies in Serum, But Not in CSF, Distinguish Multiple Sclerosis From Other Neurological Disorders. J. Neuroimmune Pharmacol. 17, 526–537. https://doi.org/10.1007/s11481-021-10048-x.

42. Buckner, C.M., Moir, S., Ho, J., Wang, W., Posada, J.G., Kardava, L., Funk, E.K., Nelson, A.K., Li, Y., Chun, T.-W., and Fauci, A.S. (2013). Characterization of Plasmablasts in the Blood of HIV-Infected Viremic Individuals: Evidence for Nonspecific Immune Activation. J. Virol. 87, 5800–5811. https://doi.org/10.1128/jvi.00094-13.

43. Kardava, L., Sohn, H., Youn, C., Austin, J.W., Wang, W., Buckner, C.M., Justement, J.S., Melson, V.A., Roth, G.E., Hand, M.A., et al. (2018). IgG3 regulates tissue-like memory B cells in HIV-infected individuals. Nat. Immunol. 19, 1001–1012. https://doi.org/10.1038/s41590-018-0180-5.

44. Perelini, F., Agnew, J., Skinner, J.R., Han, D.Y., Nicholson, R., and Wilson, N. (2022). Revisiting QT prolongation in acute rheumatic fever – Relevance for hydroxychloroquine treatment. Int. J. Cardiol. 362, 93–96. https://doi.org/10.1016/j.ijcard.2022.05.053.

45. Shirota, Y., Yarboro, C., Fischer, R., Pham, T.-H., Lipsky, P., and Illei, G.G. (2013). Impact of anti-interleukin-6 receptor blockade on circulating T and B cell subsets in patients with systemic lupus erythematosus. Ann. Rheum. Dis. 72, 118–128. https://doi.org/10.1136/annrheumdis-2012-201310.

46. Kirvan, C.A., Canini, H., Swedo, S.E., Hill, H., Veasy, G., Jankelow, D., Kosanke, S., Ward, K., Zhao, Y.D., Alvarez, S., et al. (2022). IgG2 rules: N-acetyl-β-D-glucosamine-specific IgG2 and Th17/Th1 cooperation may promote the pathogenesis of acute rheumatic heart disease and be a biomarker of the autoimmune sequelae of Streptococcus pyogenes. Front. Cardiovasc. Med. 9, 919700. https://doi.org/10.3389/fcvm.2022.919700.

47. Happonen, L., Hauri, S., Svensson Birkedal, G., Karlsson, C., de Neergaard, T., Khakzad, H., Nordenfelt, P., Wikström, M., Wisniewska, M., Björck, L., et al. (2019). A quantitative Streptococcus pyogenes-human protein-protein interaction map reveals localization of opsonizing antibodies. Nat. Commun. 10, 2727. https://doi.org/10.1038/s41467-019-10583-5.

48. van Zelm, M.C. (2014). B cells take their time: sequential IgG class switching over the course of an immune response? Immunol. Cell Biol. 92, 645–646. https://doi.org/10.1038/icb.2014.48.

49. Walkinshaw, D.R., Wright, M.E.E., Mullin, A.E., Excler, J.-L., Kim, J.H., and Steer, A.C. (2023). The Streptococcus pyogenes vaccine landscape. NPJ Vaccines 8, 16. https://doi.org/10.1038/s41541-023-00609-x.

50. Proctor, E.-J., Frost, H.R., Satapathy, S., Botquin, G., Urbaniec, J., Gorman, J., De Oliveira, D.M.P., McArthur, J., Davies, M.R., Botteaux, A., et al. (2024). Molecular characterisation of the interaction between human IgG and the M-related proteins from Streptococcus pyogenes. J. Biol. Chem. 300, 105623. https://doi.org/10.1016/j.jbc.2023.105623.

51. Surve, N.Z., Kerkar, P.G., Deshmukh, C.T., Nadkar, M.Y., Mehta, P.R., Ketheesan, N., Sriprakash, K.S., and Karmarkar, M.G. (2021). A longitudinal study of antibody responses to selected host antigens in rheumatic fever and rheumatic heart disease. J. Med. Microbiol. 70, 001355. https://doi.org/10.1099/jmm.0.001355.

52. Jones, S., Moreland, N.J., Zancolli, M., Raynes, J., Loh, J.M.S., Smeesters, P.R., Sriskandan, S., Carapetis, J.R., Fraser, J.D., and Goldblatt, D. (2018). Development of an opsonophagocytic killing assay for group a streptococcus. Vaccine 36, 3756–3763. https://doi.org/10.1016/j.vaccine.2018.05.056.

53. McGregor, R., Paterson, A., Sharma, P., Chen, T., Lovell, J.R., Carlton, L.H., Steer, A.C., Osowicki, J., Loh, J.M.S., and Moreland, N.J. (2023). Naturally acquired functional antibody responses to group A Streptococcus differ

between major strain types. mSphere *8*, e0017923. https://doi.org/10.1128/msphere.00179-23.

54. Whitcombe, A.L., McGregor, R., Craigie, A., James, A., Charlewood, R., Lorenz, N., Dickson, J.M., Sheen, C.R., Koch, B., Fox-Lewis, S., et al. (2021). Comprehensive analysis of SARS-CoV-2 antibody dynamics in New Zealand. Clin. Transl. Immunol. *10*, e1261. https://doi.org/10.1002/cti2.1261.

55. Whitcombe, A.L., Hanson-Manful, P., Jack, S., Upton, A., Carr, P.A., Williamson, D.A., Baker, M.G., Proft, T., and Moreland, N.J. (2020). Development and evaluation of a new triplex immunoassay that detects Group A Streptococcus antibodies for the diagnosis of rheumatic fever. J. Clin. Microbiol. *58*, 10–1128. https://doi.org/10.1128/jcm.00300-20.

56. Rohart, F., Gautier, B., Singh, A., and Lê Cao, K.A. (2017). mixOmics: An R package for 'omics feature selection and multiple data integration. PLoS Comput. Biol. *13*, e1005752. https://doi.org/10.1371/journal.pcbi.1005752.

STAR★METHODS

KEY RESOURCES TABLE

REAGENT or RESOURCE	SOURCE	IDENTIFIER
Antibodies		
R-Phycoerythrin Goat Anti-Human Serum IgA	Jackson ImmunoResearch Labs	Cat# 109-115-011; RRID:AB_2337674
Mouse Anti-Human IgM-PE (clone SA-DA4) R-Phycoerythrin	SouthernBiotech	Cat# 9020-09; RRID:AB_2796577
R-Phycoerythrin F(ab')₂ Fragment Donkey Anti-Human IgG	Jackson ImmunoResearch Labs	Cat# 709-116-098; RRID:AB_2340519
Mouse Anti-Human IgG1 Hinge-PE (clone 4E3)	SouthernBiotech	Cat# 9052-09; RRID:AB_2796621
Mouse Anti-Human IgG2 Fc-PE (clone HP6002)	SouthernBiotech	Cat# 9070-09; RRID:AB_2796639
Mouse Anti-Human IgG3 Hinge-PE (clone HP6050)	SouthernBiotech	Cat# 9210-09; RRID:AB_2796701
Mouse Anti-Human IgG4 Fc-PE (clone HP6025)	SouthernBiotech	Cat# 9200-09; RRID:AB_2796693
Goat Anti-Human IgG H&L (HRP)	Abcam	Cat# ab6858; RRID:AB_955433
Mouse Anti-Human IgG1 Fc-HRP (clone HP6001)	SouthernBiotech	Cat# 9054-05; RRID:AB_2796627
Mouse Anti-Human IgG1 Hinge-HRP (clone 4E3)	SouthernBiotech	Cat# 9052-05; RRID:AB_2796619
Mouse Anti-Human IgG3 Hinge-HRP (clone HP6050)	SouthernBiotech	Cat# 9210-05; RRID:AB_2796699
Bacterial and virus strains		
E. coli BL21(DE3) pLysS	ThermoFisher	Cat# C607003
Biological samples		
Pediatric sera from ARF patients	Baker et al. 2022[25]	N/A
Pediatric sera from healthy controls	Baker et al. 2022[25]	N/A
Pediatric sera from pharyngitis patients	Bennett et al. 2022[26]	N/A
Peripheral blood mononuclear cells	This manuscript	N/A
Chemicals, peptides, and recombinant proteins		
recombinant *S. pyogenes* leucine-rich repeat domain-containing protein (Spy0843)	Whitcombe et al. 2022[29]	N/A
recombinant streptococcal C5a peptidase (SCPA)	Whitcombe et al. 2022[29]	N/A
recombinant *S. pyogenes* cell envelope protease (SpyCEP)	Kindly provided by the GSK Vaccine Institute for Global Health (GVGH)	N/A
recombinant *S. pyogenes* adhesion and division protein (SpyAD)	Kindly provided by the GSK Vaccine Institute for Global Health (GVGH)	N/A
recombinant Streptolysin O (SLO)	Whitcombe et al. 2022[29]	N/A
recombinant deoxyribonuclease B (DNaseB)	Whitcombe et al. 2022[29]	N/A
recombinant *S. pyogenes* nuclease A (SpnA)	Whitcombe et al. 2022[29]	N/A
recombinant Group A Carbohydrate (GAC)	Kindly provided by the GSK Vaccine Institute for Global Health (GVGH)	N/A
recombinant M6	Jones et al. 2018[52]	N/A
recombinant M53	McGregor et al. 2023[53]	N/A
recombinant M_C2_C3	This manuscript	N/A
AlbumiNZ™ Bovine Albumin Low IgG, ≥97%	MP Biomedicals	Cat# 199897
Critical commercial assays		
Luminex Human Discovery Assay	R&D Systems	cat# LXSAHM
MILLIPLEX® MAP Human Isotyping Magnetic Bead Panel	Merk Millipore	cat# HGAMMAG-301K
MILLIPLEX Human Complement Panel 2	Merk Millipore	cat# HCMP2MAG-19K
CRP (C- reactive protein) ELISA	Tecan	cat# EU59131

Continued

REAGENT or RESOURCE	SOURCE	IDENTIFIER
Software and algorithms		
Belysa Immunoassay Curve Fitting software, version 1.2.0	Merck	https://www.sigmaaldrich.com/NZ/en/services/software-and-digital-platforms/belysa-immunoassay-curve-fitting-software
GraphPad Prism, version 10.0.3	Dotmatics	https://www.graphpad.com/features
xPonent 4.3	DiaSorin	https://int.diasorin.com/en/luminex-ltg/reagents-accessories/software
R (version 4.2.1)	Open-source software	https://www.r-project.org/
R studio (version 2023.09.0 + 463)	Posit	https://posit.co/downloads/
Other		
MagPlex microspheres	Luminex Corporation	Cat # MC100xx-01
MagPlex-Avidin microspheres	Luminex Corporation	Cat # MA-B0xx-01

RESOURCE AVAILABILITY

Lead contact

Further information and requests for resources and reagents should be directed to the lead contact, Assoc. Prof. NJ Moreland (n.moreland@auckland.ac.nz).

Materials availability

This study did not generate new unique materials, which cannot be obtained from commercial sources.

Data and code availability

The data reported in this study cannot be deposited in a public repository due to the ethical approval and data sovereignty principles under which these samples were obtained. This paper does not report original code. Any information required to re-analyse the data is available from the lead contact upon request. These requests must comply with ethical approval and associated data sovereignty principles from which the samples were obtained.

EXPERIMENTAL MODEL AND STUDY PARTICIPANT DETAILS

Participants were recruited as part of two case-control studies approved by the New Zealand Health and Disability Ethics Committee, with written informed consent obtained from all participants or their parents/guardians. Demographic characteristics of study participants are shown (Table 1). Sera of ARF cases (*n* = 60) and matched healthy controls (*n* = 30) were obtained as part of the Rheumatic Fever Risk Factor study (ethics ref. 14/NTA/53)[25] between 2014 and 2017. ARF cases were diagnosed according to the New Zealand modification of the Jones Criteria,[27] and sera were collected during hospital admission. Healthy individuals were matched with cases by age, prioritized ethnicity, socioeconomic deprivation and region, followed by sex where possible. Exclusion criteria for healthy controls for this study included: a self-reported recent sore throat or skin infection; a GAS-positive throat swab indicative of asymptomatic carriage; or positive clinical streptococcal serology, as detailed (Figure S1). GAS pharyngitis control sera (*n* = 30) was collected as part of a prospective GAS disease incidence study (ethics ref. 17/NTA/262), conducted between 2018 and 2019.[26] Inclusion criteria for this study included a GAS-positive throat swab following presentation to primary care with pharyngitis and availability of both acute (collected a median 6 (IQR 5–7) days post-symptom onset) and convalescent sera (collected a median 31 (IQR 29–37) days post-symptom onset) as shown (Figure S1).

METHOD DETAILS

Circulating analyte quantification

Cytokines were measured using a custom bead-based multiplex assay (Luminex Human Discovery Assay) according to the manufacturer's instructions with a serum dilution of 1:2. Bulk IgA, IgG1, IgG3 and C4 were quantified using bead-based assays (Merck Millipore) as previously described.[23] All bead-based assays were run on a Luminex200 instrument (Luminex Corporation) and analyzed with Belysa Immunoassay Curve Fitting software (Version 1.2.0, Merck). C-reactive protein (CRP) was quantified by ELISA (Tecan) and absorbance units were converted to μg/mL according to the manufacturer's instructions with GraphPad Prism (version 10.0.3, GraphPad Software).

Primary cell culture assays

Primary cell culture assays with peripheral blood mononulcear cells (PBMCs) were adapted from a previously published protocol.[17] PBMCs from three ARF cases were collected as part of a separate ARF study from patients during hospital admission (ethics ref. 20/NTB/163) and compared to three healthy adult lab donors as controls (ethics reference AH24859). Cells cultured in Iscove's Modified Dulbecco's Medium supplemented with 10% fetal bovine serum, 1% penicillin-streptomycin and 0.1% fungizone. Supernatants were aspirated on day 1 and day 4 and stored at −80°C until use. Cytokines secreted by the cells were measured using a custom four-plex assay (Human Luminex Discovery Assay) as described above.

Group A Streptococcus Luminex assays

Antibody responses to conserved GAS antigens were measured using an 8-plex bead-based assay comprising: *S. pyogenes* leucine-rich repeat domain-containing protein (Spy0843/LRRP); streptococcal C5a peptidase (SCPA), *S. pyogenes* cell envelope protease (SpyCEP), *S. pyogenes* adhesion and division protein (SpyAD), the Group A Carbohydrate (GAC), Streptolysin O (SLO), deoxyribonuclease B (DNaseB), and *S. pyogenes* nuclease A (SpnA).[29] Protein antigens were expressed and coupled to MagPlex microspheres (Luminex Corporation) as previously described,[29] while the GAC coupling method was modified. Purified biotinylated GAC was kindly provided by the GSK Vaccine Institute for Global Health (GVGH) and coupled to MagPlex-Avidin microspheres according to the manufacturer's instructions. In brief, magnetic MagPlex-Avidin beads were washed three times in PBS, 1% BSA prior to the addition of 5 ug GAC per 1×10^6 beads and incubation for 30 min at room temperature. Antigen-coupled beads were washed, enumerated, and stored in PBS, 1% BSA, 0.05% sodium azide at 4°C. Substitution of the biotin-GAC in place of poly-L-lysine coupled GAC did not alter assay performance, with $R^2 \geq 0.99$ between assays for all other antigens.

Sera were diluted 1:600 (IgG2, IgG3, IgG4 and IgM), 1:1000 (IgG1 and IgA) or 1:8000 (total IgG) in assay buffer (PBS pH 7.4, containing 1% bovine serum albumin) and incubated with the 8-plex microsphere cocktail for 35 min at 800 rpm, prior to three washes with assay buffer (BioTek 50 TS plate washer). For detection, beads were incubated with phycoerythrin (PE) labeled anti-human IgA, IgM, IgG, IgG1, IgG2, IgG3, or IgG4 for 35 min at 800 rpm followed by two additional washes in assay buffer as per previously developed protocols.[54] Beads were then analyzed on a Luminex200 system (Luminex Corporation) with xPonent 4.3 software. Background fluorescence values from no-serum controls were subtracted to give net median fluorescence intensity (MFI) values.

Group A Streptococcus ELISA

Recombinant SLO, M6 and M53 were expressed using *Escherichia coli* and purified as previously described.[52,53,55] The M_C2_C3 fragment sequence, representing the conserved C2-C3 repeat region of the GAS M protein was based on the M12:GAS9429 protein (N368 to Q433) and extended with two additional C-terminal tryptophan residues to enable UV detection during purification. The sequence was commercially synthesized, cloned into pGEX-4T-3 (Genscript) and expressed in *E. coli* BL21(DE3) pLysS with an N-terminal GST-tag. Bacteria were cultured at 37°C until exponential phase, protein expression was induced with 1 mM Isopropyl ß-D-1-thiogalactopyranoside (IPTG), and bacteria further cultured for 16 hrs at 18°C. M_C2_C3 purification from the bacterial cell pellet involved Glutathione Sepharose 4B resin affinity separation, GST-tag cleavage with thrombin (0.2 U/μL, MP Biomedical) followed by size exclusion chromatography. M_C2_C3 was determined to be >95% pure by SDS-PAGE, and identity was confirmed by fingerprint mass spectrometric analysis (University of Auckland Mass Spectrometry facility).

Subclass-specific antibody responses against SLO, M6, M53 and M_C2_C3 were determined in enzyme-linked immunosorbent assays (ELISAs) as published.[23] Briefly, antigens were coated at 2 ug/mL in PBS and wells blocked with PBS, 0.1% Tween 20 (PBS-T) substituted with 5% skim milk powder. Sera was diluted 1:1000 (IgG1 and IgG3) or 1:5000 (IgG) and bound antibodies were detected with HRP-labelled anti-human IgG, IgG1 (IgG1 Fc and IgG1 Hinge mixed 1:1 (v/v)), and IgG3 on a BioTek 800 TS Absorbance Reader. Absorbance readings were converted to EU in GraphPad Prism (version 9.3.1) using an 8-point standard curve constructed with positive control sera and included on every plate. The lowest dilution (1:500) on the standard curve was designated 500 EU, whereas the highest dilution (1:1,093,500) was designated 0.228 EU.

QUANTIFICATION AND STATISTICAL ANALYSIS

All analysis and graphing was conducted in R (version 4.2.1) with R studio (version 2023.09.0 + 463) using the following packages: tidyverse, package suite, rstatix, mixOmics, ggpubr, Hmisc, corrplot and pROC. For data that were log transformed the following equation was used; $y = log10(x+1)$, where x is the data and y is the log-transformed data presented. All boxplots represent the median concentration and the third (Q3) and first quartiles (Q1) with whiskers extending to the maximum and minimum values within 1.5 times the interquartile range (IQR). Unless otherwise stated non-paired t-tests were carried out with Holm-Bonferroni adjustment for multiple comparisons. Significance levels are indicated as follows: $*p < 0.05$, $**p < 0.01$, $***p < 0.001$, and $****p < 0.0001$. No participants were excluded from the analyses, thus numbers used in each group for statistical analyses are as depicted in demographics table (Table 1); ARF $n = 60$, healthy control $n = 30$ and GAS-pharyngitis group $n = 30$.

PLS-DA was conducted in the mixOmics package[56] in R with two latent variables. To assess model performance and over-fitting, K-fold cross-validation was carried out with 5-folds, repeated 100 times. The BER, important due to the unequal numbers in the study groups, was calculated using the centroid distance measure.

The network plot was constructed using log-transformed data in the igraph package in R by combining all quantified measurements. Where there was duplicated data (SLO, measured in both ELISA and Luminex) Luminex data were retained. A Pearson correlation was conducted and only significant ($p < 0.05$ after Holm-Bonferroni adjustment) and strong correlations (absolute Pearson's correlation coefficient >0.6) were retained. An adjacency matrix based on Pearson correlation coefficients was generated where nodes represent individual markers from the combined datasets. Edges between nodes correspond to significant correlations, with thickness and color proportional to the strength of each relationship. The final visualization excluded isolated nodes, ensuring that only markers with at least one significant strong correlation were displayed and was plotted using the force-directed Fruchterman-Reingold algorithm to position nodes with as few crossing edges as possible.